

Effect of annealing atmosphere on LiMn_2O_4 for thin film Li-ion Batteries from aqueous Chemical Solution Deposition.

Received 00th January 20xx,
Accepted 00th January 20xx

G. Maino,^a J. D'Haen^b, F. Mattelaer^c, C. Detavernier^c, A. Hardy^{a,d} and M. K. Van Bael^{a,d}

DOI: 10.1039/x0xx00000x

www.rsc.org/

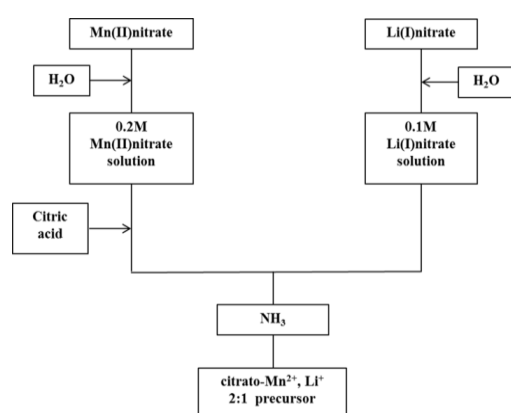


Figure S1: Synthesis scheme of the aqueous precursor solution

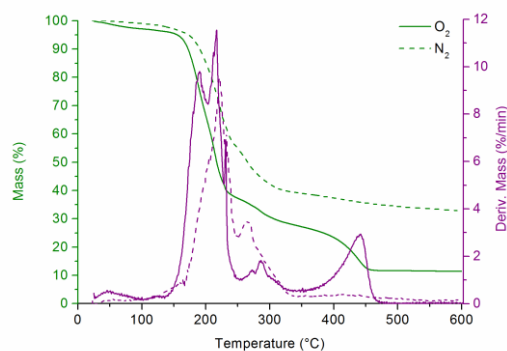
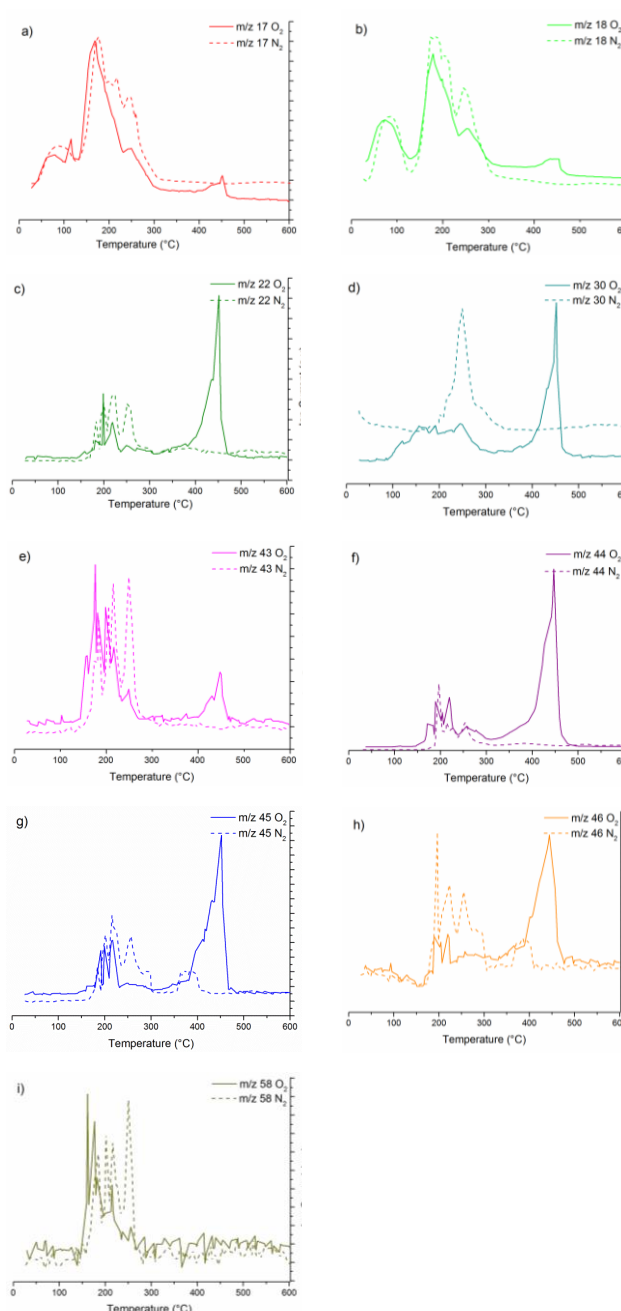


Figure S2: a) TGA (Mass %), DTG (Derivative of mass) analysis of the dried citrate- Mn^{2+} , Li^+ precursor gel. The analyses are performed in O_2 (solid line) and N_2 (dashed line).



^aUHasselt – Hasselt University, Institute for materials Research (IMO-IMOMEc), Inorganic and Physical Chemistry, Agoralaan, 3590 Diepenbeek, Belgium

^bHasselt University, Institute for Materials Research, Wetenschapspark 1, B-3590 Diepenbeek, Belgium

^cGent University, Department Solid State Sciences, Krijgslaan 281 S1, 9000 Gent (Belgium)

^dimec, division imomec, 3590 Diepenbeek, Belgium

Figure S3 (a-i): TGA-MS profiles of the dried citrate- Mn^{2+}, Li^+ precursor gel at 60°C, recorded in N_2 and O_2 at a heating rate of 10°C/min. Ions with m/z 17 (OH^+ , NH_3^+) and 18 (H_2O^+ , NH_4^+) are fragments related to water and ammonia. Ions with m/z 22 (CO_2^+), 44 (CO_2^+ , $H_2N-C=O^+$, $C_3H_8^+$) and 45 ($^{13}CO_2^+$) are fragments related to the carboxylate groups. Ions with m/z 30 (NO^+ , $C_2H_6^+$, $H_2N=CH_2^+$), 43 ($HNCO^+$, $C_2H_7^+$), 44 (CO_2^+ , $H_2N-C=O^+$), $C_3H_8^+$) are fragments related to the interaction between carboxylic acid groups and NH_3 . Ions with m/z 46 (NO_2^+ , $C_2H_5OH^+$) and 58 ($C_3H_6O^+$) together with previous ones (m/z 30, 43, 44) are fragments related to the citrate's skeleton. Only the most relevant fragments are shown and cited in the article. Note that each sub-figure has its own ion current scale.

It can be noted that fragments 30 (NO^+ , $C_2H_6^+$, $H_2N=CH_2^+$), 43 ($HNCO^+$, $C_2H_7^+$) and 44 (CO_2^+ , $H_2N-C=O^+$) evolve at lower temperature in O_2 atmosphere (180-190°C) motivating partially the faster mass lost in oxidative atmosphere around the same temperature.

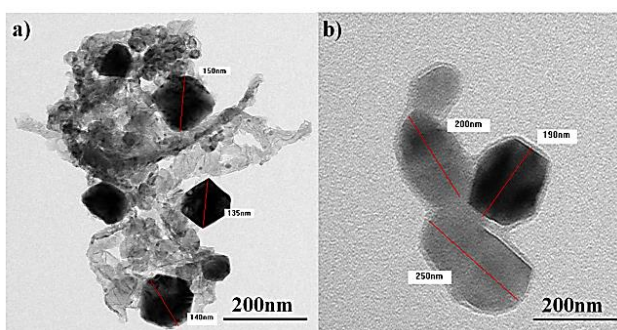


Figure S4: TEM images of powders obtained after calcining dried precursor gels at 450 °C for 1h in a) N_2 and b) O_2

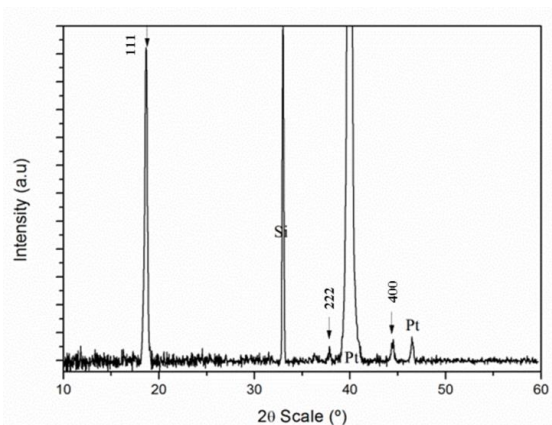


Figure S5: XRD of film on $Si/SiO_2/TiN/Pt$ substrate, heated at 450°C for 1h in N_2 . Arrow represents $LiMn_2O_4$ face centered cubic spinel phase (JCPDS 89-0117).

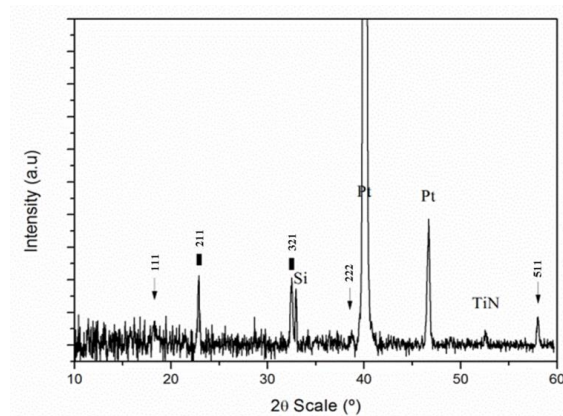


Figure S6: XRD of film on $Si/SiO_2/TiN/Pt$ substrate, heated at 450°C for 1h in O_2 . Arrow represents $LiMn_2O_4$ face centered cubic spinel phase (JCPDS 89-0117), square represents gamma Mn_2O_3 tetragonal (JCPDS 06-0540).

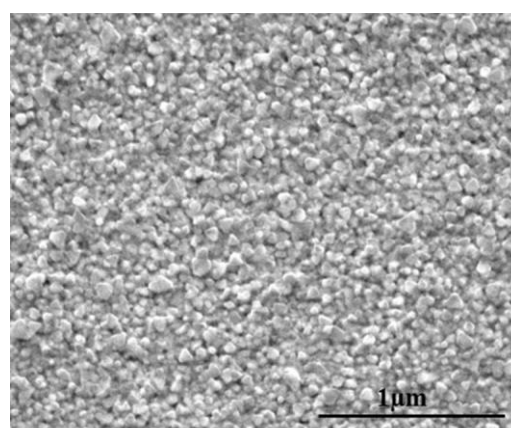


Figure S7: SEM Pictures of films on $Si/SiO_2/TiN/Pt$, annealed in N_2 at 450°C

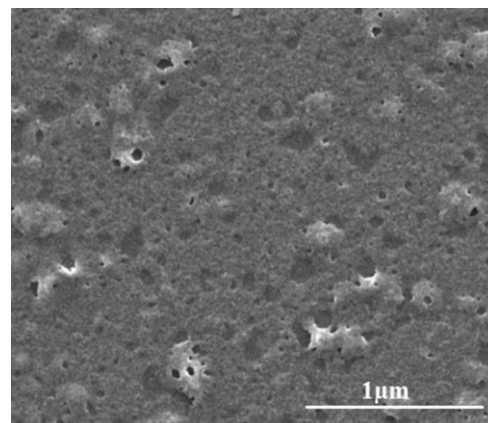


Figure S8: SEM Pictures of films on $Si/SiO_2/TiN/Pt$, annealed in O_2 at 450°C for 1h at 10°C/min.

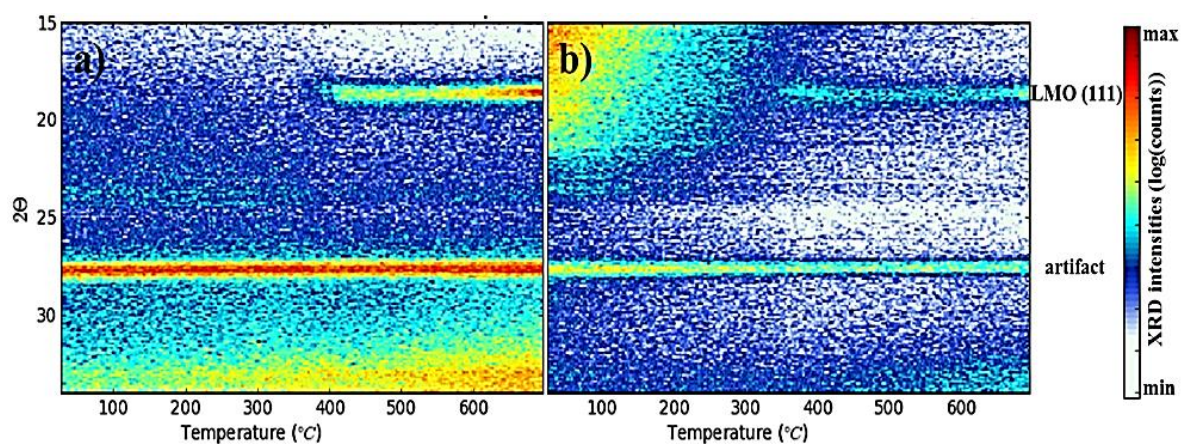


Figure S9: In-situ XRD of spincoated films on Si substrate, recorded in N_2 and O_2 at a heating rate of $12\text{ }^\circ\text{C}\cdot\text{min}^{-1}$. The reflection at $27,5^\circ 2\theta$ originates from a detector artifact.

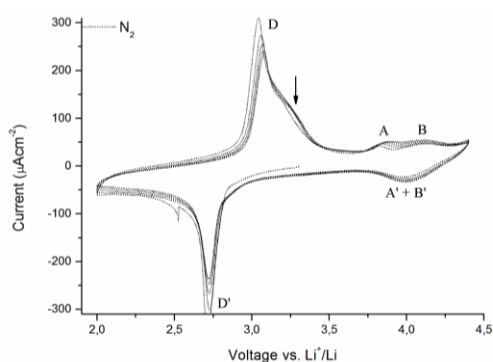


Figure S10: Cyclic Voltammogram (first 5 cycles, $10\text{mV}/\text{sec}$) of the films onto Si/Si/SiO₂/TiN/Pt, after annealing at $800\text{ }^\circ\text{C}$ for 3h in N_2

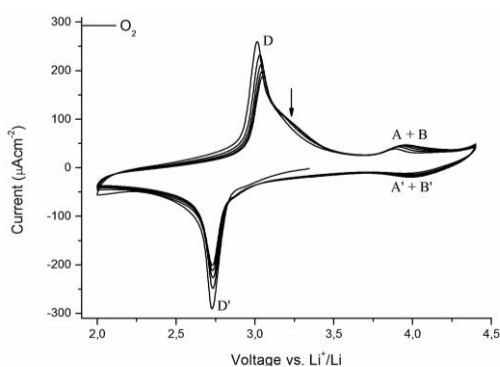


Figure S11: Cyclic Voltammogram (first 5 cycles, $10\text{mV}/\text{sec}$) of the films onto Si/Si/SiO₂/TiN/Pt, after annealing at $800\text{ }^\circ\text{C}$ for 3h in O_2